Journal of Geographical Sciences 15, 4 (2005) 439–447 ISSN: 1009–637X www.geog.cn

Distributed modeling of direct solar radiation on rugged terrain of the Yellow River Basin

ZENG Yan[1], *QIU Xinfa*[2], *LIU Changming*[3], *JIANG Aijun*[1]
(1. Jiangsu Institute of Meteorological Sciences, Nanjing 210008, China; 2. Department of Geospatial Information Sciences, Nanjing University of Information Science and Technology, Nanjing 210044, China; 3. Institute of Geographic Sciences and Natural Resources Research, CAS, Beijing 100101, China)

Abstract: Due to the influences of local topographical factors and terrain inter-shielding, calculation of direct solar radiation (DSR) quantity of rugged terrain is very complex. Based on digital elevation model (DEM) data and meteorological observations, a distributed model for calculating DSR over rugged terrain is developed. This model gives an all-sided consideration on factors influencing DSR. Using the developed model, normals of annual DSR quantity with a resolution of 1 km × 1 km for the Yellow River Basin was generated, with DEM data as the general characterization of terrain. Characteristics of DSR quantity influenced by geographic and topographic factors over rugged terrain were analyzed thoroughly. Results suggest that: influenced by local topographic factors, i.e. azimuth, slope and so on, and annual DSR quantity over mountainous area has a clear spatial difference; annual DSR quantity of sunny slope (or southern slope) of mountains is obviously larger than that of shady slope (or northern slope). The calculated DSR quantity of the Yellow River Basin is provided in the same way as other kinds of spatial information and can be employed as basic geographic data for relevant studies as well.

Key words: direct solar radiation (DSR); rugged terrain; digital elevation model (DEM); distributed model; Yellow River Basin
doi: 10.1360/gs050407

1 Introduction

Direct solar radiation (DSR) is the key component of the global radiation reaching the Earth. For the influence of terrain factors, calculation of DSR quantity of rugged terrain is considerably complex (Oliphant *et al*., 2003).

The solar radiation quantity reaching the rugged terrain is influenced by many factors such as astronomical and geographic factors (i.e. solar constant, relative sun-earth distance, solar declination, latitude, etc.), local topographic factors (i.e. azimuth, slope, terrain inter-shielding, etc.), atmospheric physical factors (i.e. atmosphere molecules, aerosol particles, etc.) and meteorological factors (i.e. cloudage, cloud varieties, etc.) (Zeng *et al*., 2003; Dozier *et al*., 1990). Throughout the literature, investigations on astronomical and geographic factors are relatively ideal, which are mainly related to the calculation of horizontal extraterrestrial solar radiation; researches on local topographic factors are mainly related to the general developed models for calculation of solar radiation on slopes and theoretical formulas for calculation of extraterrestrial solar radiation on given single slope, regardless of the influence of terrain inter-shielding effects (Zuo *et al*., 1991; Zhu, 1988). Studies on atmospheric physical factors are mainly related to models on clear sky solar radiation simulation (David, 1997; Maxwell, 1998; Iqbal, 1983). Studies on meteorological factors are mainly related to empirical models developed by solar radiation observation data of meteorological stations for horizontal solar radiation

Received: 2005-05-19 **Accepted:** 2005-08-12
Foundation: Major State Basic Research Development Program of China, No.G20000779; No.G19990436-01
Author: Zeng Yan (1972-), Ph.D. and Associate Researcher, specialized in environmental remote sensing and GIS.
E-mail: jlzengyan@sina.com

simulation (Wong *et al.*, 2001; Weng, 1997).

DSR quantity falling on a rugged terrain is not only influenced by topographical factors, such as aspect and slope of the terrain, but also influenced by inter-shielding effect caused by surrounding terrains. For the terrain inter-shielding effect changes with the sun's apparent path in the sky, the simulation of the DSR distribution on rugged terrain is very complex. In recent decades, the development of Geographical Information System (GIS) breaks a new path for rugged-terrain solar radiation simulation. Previous studies show that a distributed model, basing on DEM data, makes the simulation of solar radiation of rugged terrain possible (Qiu *et al.*, 2004; Li *et al.*, 1988; Ranzi *et al.*, 1995; Dubayah *et al.*, 1990; Bocquet, 1984; Dozier *et al.*, 1979). Using DEM data as the general characterization of terrain and GIS as data processing platform, distributed modeling of DSR quantity of rugged terrains of the Yellow River Basin was achieved.

2 Data and method

As we know, meteorological stations are usually situated at open flat with limited number, and their conventional solar radiation data only represent the horizontal observation results. Therefore, distribution of solar radiation over rugged terrain can only be got by simulation. In this paper, we use a distributed model to simulate DSR quantity distribution of rugged terrain.

Based on the theory of DSR on slopes, the calculation formula of DSR over rugged terrain was given below:

$$\frac{Q_{0\alpha\beta}}{Q_0} = \frac{Q_{b\alpha\beta}}{Q_b} \tag{1}$$

where $Q_{0\alpha\beta}$ is the extraterrestrial solar radiation (ESR) quantity of rugged terrain (ESR describes the solar radiation falling on the earth surface with no account taken of atmospheric effect); Q_0 is ESR quantity of horizontal plane; $Q_{b\alpha\beta}$ is DSR quantity of rugged terrain; and Q_b is DSR quantity of horizontal plane.

From equation (1) one can get:

$$Q_{b\alpha\beta} = Q_{0\alpha\beta}\ \frac{Q_b}{Q_0} = R_b\, Q_b = Q_{0\alpha\beta} k_b \tag{2}$$

where $R_b = \frac{Q_{0\alpha\beta}}{Q_0}$, it is the ratio of ESR quantity of rugged terrain to that of horizontal plane, it is also called conversion factor to represent the influences of terrain on DSR (Zuo *et al.*, 1991); $k_b = \frac{Q_b}{Q_0}$, it is the ratio of DSR quantity to ESR quantity of horizontal plane and termed direct transmittance to represent the influences of atmosphere on DSR (Louche *et al.*, 1991).

Given $Q_{0\alpha\beta}$, Q_0 and Q_b, using equation (2) one can get the distribution of DSR quantity of rugged terrain. Here, $Q_{0\alpha\beta}$ is calculated by a developed distributed model (Qiu *et al.*, 2004); Q_0 is calculated by theoretical formulae (Zuo *et al.*, 1991); and Q_b is simulated by meteorological data fitting statistical models①.

Meteorological data used in this study are monthly mean percentage of sunshine and the amount of clouds from 164 meteorological stations, and monthly solar radiation quantity from 35 meteorological stations (of which 35 stations have global solar radiation data and 21 have DSR data). All the meteorological stations are near or in the Yellow River Basin and their locations are shown in Figure 1. The time series of most of monitoring data is from 1960 to 2000. Before using, data quality detection is made.

① Even in mountainous area, meteorological stations are usually situated at open flat and no obstacles in certain scope. Data of them only represent the horizontal observation results. So, in this study, global solar radiation and direct solar radiation models fitted by meteorological data are all horizontal simulations.

Figure 1 Distribution of meteorological stations in and around the Yellow River Basin for the routine meteorological elements and solar radiation observation

3 Horizontal DSR (Q_b) simulation of the Yellow River Basin

3.1 Horizontal DSR (Q_b) simulation models

DSR is the key component of the global radiation reaching the Earth. They are highly correlated (Louche *et al*., 1991; Vignola *et al*., 1986). Thereafter, we construct the Q_b simulation model as:

$$Q_b = Q(1 - a)(1 - \exp[-bs^c/(1 - s)]) \tag{3}$$

where Q is global solar radiation quantity of horizontal plane; s is percentage of sunshine; and a, b and c are empirical coefficients.

Equation (3) has clear physical meaning. Namely, in complete gloomy weather, $s = 0$, there are no DSR and $Q_b = 0$; in complete clear weather, $s \to 1$, the solar radiation reaching the Earth is mainly comprised of DSR and Q_b approaches to the maximum, i.e. $Q_b \to Q(1 - a)$.

In equation (3), empirical coefficients a, b and c can be fitted by observational data. For the number of stations that have DSR observational data is small, DSR data of all the stations were integrated to fit the model. In order to analyze the changing characters of a, b and c with time and space, different datasets were used and the related fitted models of Q_b are called unified model and monthly model respectively. Their meanings are as follows.

(1) Unified model: Q_b observational data of all stations are used to fit the model (model number: 1).

(2) Monthly model: Q_b observational data of all stations of the same month are used to fit the model (model number: 12).

The statistics of different models are shown in Table 1.

In Table 1, the statistical indices are square of correlation coefficient (R^2), Mean Absolute Bias Error (MABE) and Mean Absolute Relative Bias Error (MARBE).

From Table 1 one can find that: having considered the empirical coefficients changing characters with time, monthly models can improve the simulation accuracy of Q_b effectively. Thereby, for stations having global solar radiation data, we can use the monthly model to simulate Q_b. Table 2 gives coefficients and statistics of monthly models for Q_b simulation.

For the meteorological stations that have global solar radiation (Q) data are limited and most of the stations only have routine meteorological data, i.e. percentage of sunshine and the amount of clouds, using equation (3) to simulate Q_b needs to determine Q first.

Table 1 Statistics of different models for horizontal direct solar radiation simulation

Model	Model Number	R^2	MABE (MJ m^{-2} day^{-1})	MARBE (%)
Unified Model	1	0.92	0.83	10.85
Monthly Model	12	0.89	0.72	9.45

Note: For monthly model the statistical figures are the mean.

3.2 Horizontal global solar radiation (Q) simulation models

Volume of studies show that horizontal global solar radiation (Q) and percentage of sunshine (s) have a good correlation and their linear equation can be given as follows (Wong *et al.*, 2001; Weng, 1997):

$$Q = Q_0(a_G + b_G \cdot s) \quad (4)$$

where a_G, b_G are empirical coefficients.

Table 2 Coefficients and statistics of monthly models for the horizontal direct solar radiation simulation

Month	a	b	c	R^2	n
1	0.3192	0.9659	0.6107	0.88	527
2	0.3148	0.7158	0.3111	0.88	539
3	0.2917	0.5367	0.1162	0.85	543
4	0.3529	0.6715	0.1846	0.83	548
5	0.3275	0.6443	0.0394	0.86	541
6	0.3178	0.8619	0.3426	0.89	544
7	0.3113	1.0139	0.5062	0.90	550
8	0.2612	0.7669	0.2949	0.91	545
9	0.2813	0.8490	0.3292	0.92	541
10	0.2654	0.7654	0.3125	0.93	541
11	0.2826	0.7876	0.3466	0.89	534
12	0.2925	0.8179	0.4794	0.90	519

n is the sample length

Physical meaning of equation (4) is that: in complete gloomy weather, $s = 0$, $Q \rightarrow Q_0 a_G$, the global solar radiation (Q) reaching the Earth approaches to the minimum; in complete clear weather, $s \rightarrow 1$, $Q \rightarrow Q_0(a_G + b_G)$, the global solar radiation (Q) reaching the Earth approaches to the maximum. a_G and b_G have no direct relation with terrain and are mainly related to climatic condition (e.g. the amount of cloud) and atmospheric transparency. For reasons given above and combined the consideration that the Q simulation model is linear and the number of stations which have Q data larger than that of Q_b, the fitted models for Q simulation are as follows:

(1) Unified model: Q observational data of all stations are used to fit the model (model number: 1).

(2) Monthly model: Q observational data of all stations of the same month are used to fit the model (model number: 12).

(3) Single station model: all the Q observational data of a single station are used to fit the model (model number: 35).

(4) Monthly single station model: Q observational data of the same month of a single station are used to fit the model (model number: $35 \times 12 = 420$).

The statistics of different models are given in Table 3.

The difference between monthly model and unified model or monthly single station model and single station model is that the former considered the changing characters of empirical coefficients with time and the latter is not. The difference between monthly single station model and monthly model or single station model and unified model is that the former considered the changing characters of empirical coefficients with space and the latter is not. From Table 3 one can find that: considering the changing characters of empirical coefficients with space will improve the fitting accuracy of Q (i.e. MARBE) by about 2.7% -3.0% and considering the changing characters of empirical coefficients with time will improve the fitting accuracy of Q by about 0.2%-0.5%. Having considered both the changing characters of empirical coefficients with time and space, the monthly single station model has the highest fitting accuracy of Q. Nevertheless, for the sample quantity of it is low, the stability of this kind of model is also low (i.e. the square of correlation coefficient R^2 is low). Combining all the considerations above, we use the single station model to simulate Q. Coefficients of it for Q simulation can be found in Table 4.

Table 3 Statistics of different models for the horizontal global solar radiation simulation (Different models are established based on different datasets as input.)

Model	Model Number	R^2	MABE (MJ m^{-2} day^{-1})	MARBE (%)
Unified Model	1	0.91	1.24	8.64
Monthly Model	12	0.70	1.22	8.47
Single Station Model	35	0.95	0.85	5.97
Monthly Single Station Model	420	0.60	0.77	5.42

Note: For monthly model the statistical figures are the mean.

Table 4 Coefficients in the horizontal global solar radiation simulation models of 35 stations (Each model is established based on single station dataset as input.)

Station_ID	Station Name	a_G	b_G	Station_ID	Station Name	a_G	b_G
52267	Ejinaqi	0.3046	0.4552	53963	Houma	0.1886	0.5058
52533	Jiuquan	0.2931	0.4269	54527	Tianjin	0.1362	0.6018
52681	Minqin	0.2021	0.5316	54764	Fushan	0.1598	0.5429
52754	Gangcha	0.1549	0.6814	54765	Yantai	0.1017	0.6044
52818	Golmud	0.2739	0.5388	54823	Jinan	0.1015	0.6086
52866	Xining	0.1810	0.6025	54936	Juxian	0.2561	0.4200
52889	Lanzhou	0.2006	0.5001	56029	Yushu	0.1835	0.6388
53068	Erenhot	0.1924	0.6000	56043	Golog	0.2225	0.5988
53336	Haliut	0.2066	0.5575	56137	Changdu	0.2205	0.5968
53463	Huhhot	0.1081	0.7082	56146	Ganzi	0.3046	0.4899
53487	Datong	0.1804	0.5888	56173	Hongyuan	0.1770	0.6579
53543	Dongsheng	0.2200	0.4892	56196	Mianyang	0.1682	0.5934
53545	Altan Xiret	0.0919	0.6641	57006	Tianshui	0.1978	0.6287
53614	Yinchuan	0.2364	0.5060	57036	Xi'an	0.2119	0.4693
53772	Taiyuan	0.1628	0.5833	57083	Zhengzhou	0.1957	0.4840
53817	Guyuan	0.1689	0.5743	57178	Nanyang	0.1860	0.4966
53845	Yan'an	0.1936	0.4667	57245	Ankang	0.1930	0.4738
53898	Anyang	0.2349	0.3798				

For the single station model considered the changing characters of empirical coefficients with space, the spatial distribution of them should be got first. Using the fitted empirical coefficients of the 35 stations (Table 4), spatial distribution of the empirical coefficients (a_G, b_G) for Q simulation is generated by interpolation method of Inverse Distance Weight (IDW). According to the spatial distribution map, empirical coefficients for Q simulation of the 164 meteorological stations are got.

Substitute equation (4) into equation (3) gives equation (5):

$$Q_b = Q_0(a_G + b_G \cdot s)\ (1 - a)(1 - \exp[-bs^c/(1 - s)]) \tag{5}$$

Using equation (5) to simulate Q_b only needs data of percentage of sunshine as input.

Statistics show that using equation (5) to simulate Q_b the MABE is 0.90 MJ m^{-2} day^{-1} and the MARBE is 11.78%.

3.3 Spatial distribution of horizontal DSR (Q_b) in the Yellow River Basin

Using the developed models, monthly Q_b quantities of all meteorological stations from 1960 to 2000 are got. Then, using IDW interpolation method, monthly Q_b quantity with a resolution of 1 km×1 km are generated. In order to make the interpolation accuracy as high as possible and in view of the fact that the station density has much influence on the interpolation accuracy, three kinds of Q_b datasets are used in the interpolation process. They are:

(1) Direct Q_b observation dataset of some meteorological stations, no estimation error.

(2) Q_b simulated dataset by observation data of Q of some meteorological stations (i.e. using equation (3)).

(3) Q_b simulated dataset by observation data of percentage of sunshine of most of meteorological stations (i.e. using equation (5)).

4 Spatial distribution of DSR of rugged terrain of the Yellow River Basin

Using equation (2), combined with the calculated results of $Q_{0\alpha\beta}$, Q_0 and Q_b, spatial distribution of monthly DSR quantity with a resolution of 1 km × 1 km on rugged terrain ($Q_{b\alpha\beta}$) of the Yellow River Basin is generated and yearly DSR quantity is got accordingly.

Figure 2 depicts the pattern of normals of annual DSR quantity on rugged terrain of the

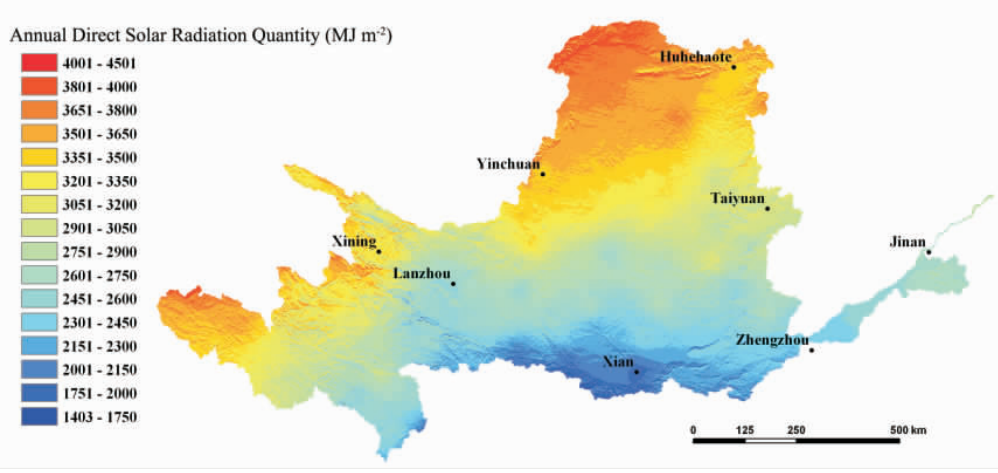

Figure 2 Distribution of normals of annual direct solar radiation quantity of 1960-2000 on rugged terrain of the Yellow River Basin

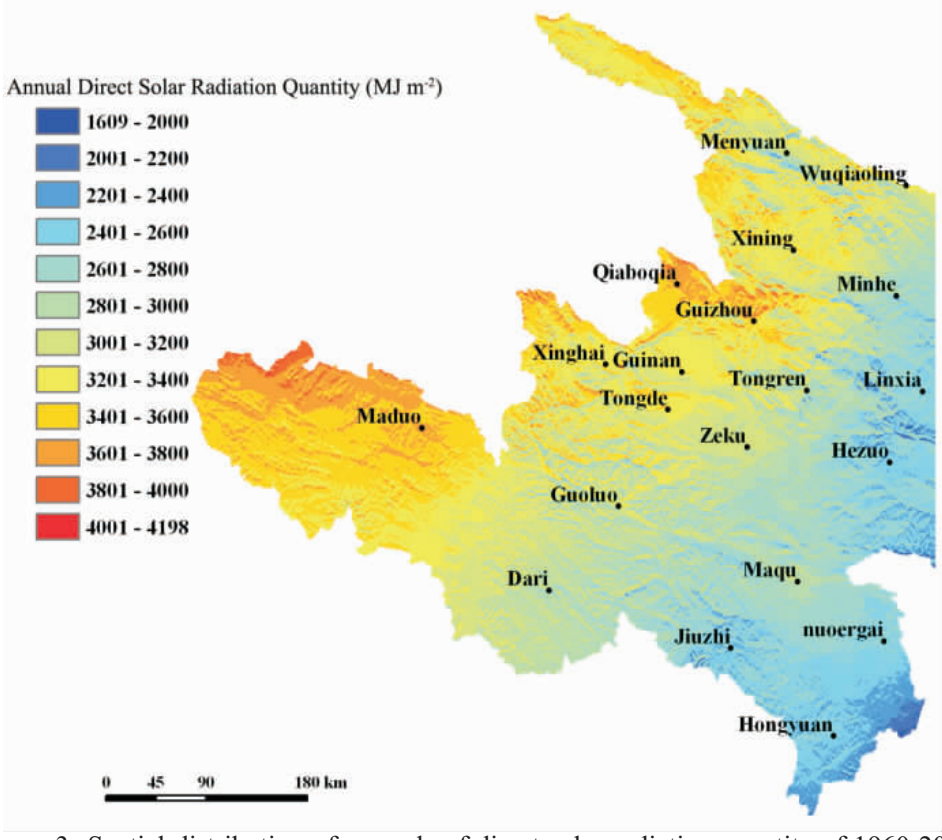

Figure 3 Spatial distribution of normals of direct solar radiation quantity of 1960-2000 in the upstream mountainous areas of the Yellow River Basin

Yellow River Basin, in which each grid value represents a mean over a 1 km^2 area. Statistics shows that normals of the average annual DSR quantity (i.e. $Q_{b\alpha\beta}$) of the Yellow River Basin is 2961 MJ m^{-2}. From Figure 2 we can find that: the annual DSR quantities in the western and northern parts of the Yellow River Basin are high and that in the eastern and southern are relatively low; Hetao Plain and Ordos Plateau have the highest DSR quantity of 3200-4500 MJ m^{-2}; Qinghai Plateau in the upstream areas has the second highest DSR quantity of 2600-3800 MJ m^{-2}; and the southeastern part has the lowest DSR quantity of 1800-2400 MJ m^{-2}. The DSR distribution pattern of the Yellow River Basin is mainly related to the facts that the southeastern part of it is full of water vapor so has high cloud cover accordingly and the western and northern parts of it are on the other hand, namely, are short of water vapor and have low cloud cover.

Figure 3 portrays DSR quantity in the mountainous upper reaches of the Yellow River Basin. From the color of the figure, one can easily find that influenced by local topographic factors, i.e. azimuth and slope, the annual DSR quantity over mountainous area has a clear spatial difference; and the annual DSR quantity of sunny slope (or southern slope) of mountains is obviously larger than that of shady slope (or northern slope).

5 Influence of topographic factors on DSR quantity of rugged terrain

From equations (1) and (2) we know that the conversion factor R_b (the ratio of ESR quantity of rugged terrains to that of flat planes) can represent the influences of terrain on DSR. For further analysis purpose, spatial distributions of R_b in the Yellow River Basin① are generated. Based on the solar radiation calculation results of the Yellow River Basin, curves of R_b verse slope or azimuth are generated (Figure 4). In Figure 4, 0° denotes north azimuth and, under a clockwise direction, 90° denote east azimuth, 180° south azimuth and 270° west azimuth.

Figure 4a shows the curves of R_b of different months verse azimuths, with latitude of 32°N and slope of 10°. In Figure 4a, one can find that the curve of January has the largest range of variation (i.e. fluctuation amplitude) and October in the next place; April and July have a relatively small range of variation. Therefore, we can draw the conclusion that in the cold half-year the effect of azimuth on DSR is larger than that of the warm half-year. In January, R_b of southward slope is obviously greater than 1, so it gets more DSR quantity than horizontal land; whereas, R_b of northward slope is obviously smaller than 1, so it gets less DSR quantity than horizontal land. In October, the pattern of the curve is similar to that of January, whereas the influence of azimuth on R_b is smaller than that of January. In April, the influence of azimuth on R_b is even smaller. In July, change of R_b with azimuth is not obvious; no matter what azimuth is, R_b approaches 1 but smaller than 1. From the intersection points of the curves one can find that no matter what month is, R_b of eastern and western slopes is always approximately equal to 1, so they get nearly the same DSR quantity as horizontal land all the year round. Furthermore, the local fluctuations in the curves denote the influence of terrain inter-shielding, which also exists in Figure 4b, Figure 4c and Figure 4d.

Figure 4b shows the curves of R_b of different latitudes verse azimuths, with month of January and slope of 10°. From Figure 4b one can find that from 32°N to 40°N, as the latitude increases, the influence of azimuth on R_b strengthens. The phenomenon also exists that R_b of the eastern and western slopes is approximately equal to 1.

Figure 4c shows the curves of R_b of different slopes verse azimuths, with latitude of 32°N and month of January. From Figure 4c one can find that from 1° to 20°, as the slope increases, the influence of azimuth on R_b strengthens. The phenomenon of R_b of the eastern and western slopes is the same as Figure 4a.

Figure 4d shows the curves of R_b of different azimuths verse slopes, with latitude of 32°N

① The Yellow River Basin is located between the Qinling Mountains and the Yinshan Mountains. Its geographic scope is 32°-42°N and 96°-119°E.

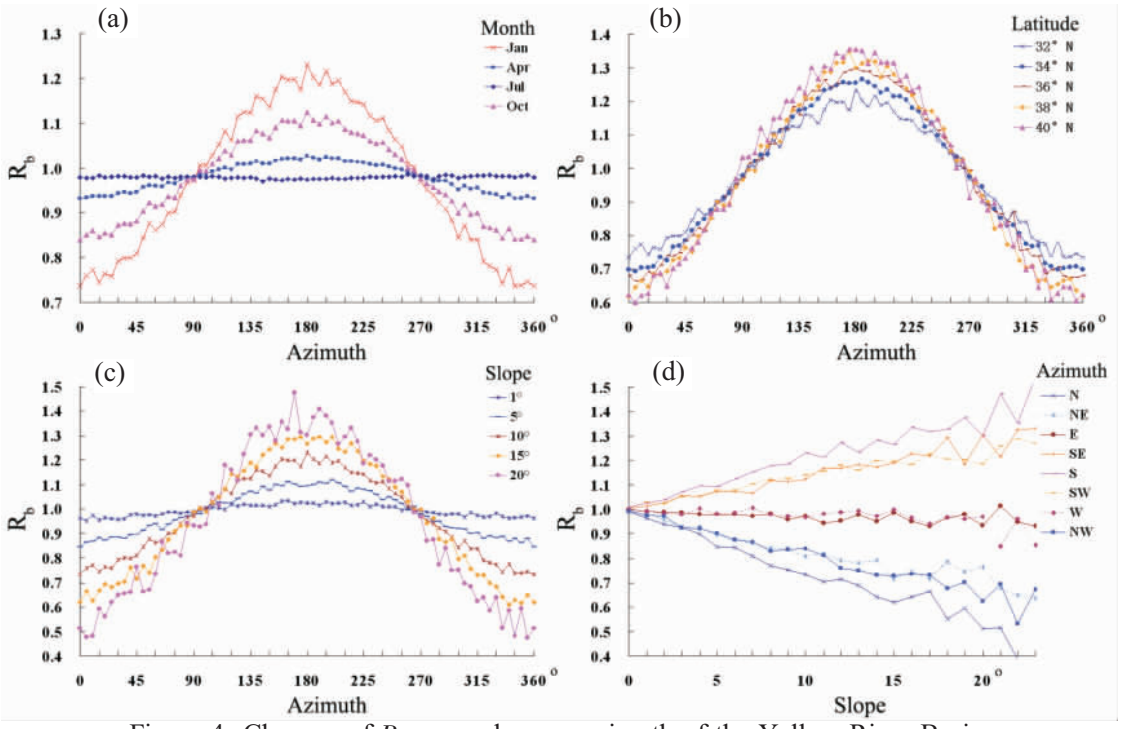

Figure 4 Changes of R_b verse slope or azimuth of the Yellow River Basin

and month of January. From Figure 4d one can find that R_b of the slopes with south, southeast and southwest azimuths is obviously greater than 1, i.e. they get more DSR quantity than horizontal land, and as the slope increases from 0° to 23°, R_b increases; R_b of the slopes with north, northeast and northwest azimuths is obviously smaller than 1, i.e. they get less DSR quantity than horizontal land, and as the slope increases from 0° to 23°, R_b decreases; R_b of the eastern and western slopes is approximately equal to 1, so they get nearly the same DSR quantity as horizontal land and as the slope changes from 0° to 23°, R_b of them has no obvious change. We can also find that: R_b of the slopes with southeast and southwest azimuths are comparative and R_b of the slope with northeast and northwest azimuths are comparative too, namely, in the same latitude area, when the slope angles are the same, the DSR quantity of the southeastern and southwestern slopes are comparative and the northeastern and northwestern slopes have the same characteristics too.

6 Conclusions

The DSR quantity reaching the rugged terrain is the compositive action results of astronomical and geographic factors, local topographic factors, atmospheric physics factors, etc. Using the developed distributed model for calculating DSR quantity of rugged terrain, all the above factors relating to sky or ground are combined effectively. Using DEM data with a resolution of 1 km × 1 km as the general characterization of terrain, combined with meteorological observations, DSR quantity with a resolution of 1 km × 1 km for the Yellow River Basin was generated. This study draws to some principal conclusions as follows:

(1) Distributed model is the key technology to achieve the simulation of solar radiation of rugged terrain.

Using DEM data as the general characterization of terrain and ESR quantity of rugged terrain as input are key means to use numerical simulation method to solve the influence of topographic factors on DSR. Using direct transmittance (k_b) to represent the influences of atmosphere on

DSR is an effective way to fully utilize the meteorological observations to simulate the influence of the sky factors on DSR. Basing on the theory of DSR on slopes to set up a distributed model of DSR of rugged terrain is the key technology to combine the sky and ground factors to achieve the simulation of DSR of rugged terrain.

(2) The influences of local topographic factors on the distribution of DSR of rugged terrain change with season and latitude.

In the winter half year with low sun elevation angle, the influence of topographical factors on DSR of rugged terrain is larger than that of the summer half year with high sun elevation angle. Furthermore, as the latitude increases (in the Yellow River Basin), the influence of topographical factors strengthens.

(3) For horizontal solar radiation simulation, empirical models fitted by appropriate dataset are more stable.

Empirical coefficients in geographic models change with space and time. In this study, using data integration technique, Q_b simulation models fitted by different datasets are analyzed thoroughly and the best stable models fitted by appropriate dataset are selected. This process is very important for the spatial expand of solar radiation and can be used for other similar elements which are changeful with time and space.

References

Bocquet G, 1984. Method of study and cartography of the potential sunny periods in mountainous areas. *Journal of Climatology*, 1(4): 587-596.

David W M, 1997. Estimation of maximum possible daily global solar radiation. *Agricultural and Forest Meteorology*, 87: 223-241.

Dozier J, Qutcalt S I 1979. An approach to energy balance simulation over rugged terrain. *Geographical Analysis*, (11): 65-85.

Dozier J, Frew J, 1990. Rapid calculation of terrain parameters for radiation modeling from digital elevation data. *IEEE Transaction on Geoscience and Remote Sensing*, 28(5): 963-969.

Dubayah R, Dozier J, Davis F W, 1990. Topographic distribution of clear-sky radiation over the Konza Prairie, Kansas, USA. *Water Resour. Res*., 26: 679-690.

Iqbal M, 1983. An Introduction to Solar Radiation. Toronto: Academic Press.

Li Zhanqing, Weng Duming, 1988. A computer model for calculating the duration of sunshine in mountainous areas. *Chinese Science Bulletin*, 33: 1624-1629.

Liu B Y H, Jordan R C, 1960. The interrelationship and characteristic distribution of direct, diffuse and total solar radiation. *Solar Energy*, 4(3): 1-19.

Louche A, Notton G, Poggi P *et al*., 1991. Correlations for direct normal and global horizontal irradiation on a French Mediterranean site. *Solar Energy*, 46(4): 261-266.

Maxwell E L, 1998. METSTAT: the solar radiation model used in the production of the NSRDB. *Solar Energy*, 62 (4): 263-279.

Oliphant A J, Spronken-Smith R A, Sturman A P *et al*., 2003. Spatial variability of surface radiation fluxes in mountainous terrain. *J. Appl. Meteor*., 42: 113-128.

Qiu Xinfa, Zeng Yan, Liu Changming *et al*., 2004. Simulation of astronomical solar radiation over Yellow River Basin based on DEM. *Journal of Geographical Sciences*, 14(1): 63-69.

Ranzi R, Rosso R, 1995. Distributed estimation of incoming direct solar radiation over a drainage basin. *Journal of Hydrology*, 166: 461-478.

Vignola F, McDaniels D K, 1986. Beam-global correlations in the Northwest Pacific. *Solar Energy*, 36 (5): 409-418.

Weng Duming, 1997. Studies on Radiation Climate of China. Beijing: China Meteorological Press. (in Chinese)

Wong L T, Chow W K, 2001. Solar radiation model. *Applied Energy*, 69, 191-224.

Zeng Yan, Qiu Xinfa, Miao Qilong *et al*., 2003. Distribution of possible sunshine durations over rugged terrains of China. *Progress in Natural Science*, 13(10): 761-764.

Zhu Zhihui, 1988. The global distribution of astronomical solar radiation on nonhorizontal surfaces. *Science in China* (Series B), 10: 1100-1110. (in Chinese)

Zuo Dakang, Zhou Yunhua, Xiang Yueqin *et al*., 1991. On Surface Radiations. Beijing: Science Press. (in Chinese)